International Conference on Applied Energy 2020
Dec. 1 - Dec. 10, 2020, Bangkok / Virtual
Paper ID: 156

Experimental investigation on temperature response and heat transfer characteristics of super-long flexible heat pipe for geothermal utilization

Hao Liu, Xiaoyuan Wang*, Yuezhao Zhu

School of mechanical and power engineering, Nanjing Tech University, Nanjing 211816, China;

ABSTRACT

A super-long flexible heat pipe (SFHP) with the total length up to 32m is experimentally tested in this work to evaluate its potential for geothermal utilization in Nanjing, China. Its evaporator section, fabricated by metal bellows, is 30m long and vertically installed in a ground drilling. The temperature response and heat transfer characteristics of SFHP were investigated. The results show that the underground temperature at the depth larger than 10m is stable in the range of 17-18℃ throughout the year. SFHP starts to operate upon the temperature at the wall of condensation section falls below 15℃. The heat transfer power of SFHP increases with decreasing temperature of cooling water. The variation of cooling water flow rate has an insignificant influence on the heat transfer power of SFHP, however its effect on the total thermal resistance is remarkable. In tests, the maximum heat transfer power is about 168.3W when the flow rate of cooling water is controlled at 600ml/min and the average temperature at 8.5℃. In addition, the higher the flow rate of cooling water, the shorter the start-up time.

Keywords: Super-long flexible heat pipe, Geothermal utilization, Temperature response, Heat transfer characteristic

NONMENCLATURE

Abbreviations	
SFHP	Super-long Flexible Heat Pipe
Symbols	
c_p	heat capacity, J/(kg K)
Q	heat exchange rate, W
R	thermal resistance, K/W
v	flow rate m^3/s
T	temperature, K
t_s	start-up time

1. INTRODUCTION

A two-phase closed thermosyphon, or refereed as the wickless heat pipe, is a passive heat transfer device, based on the phase change circulation of the internal working fluid by evaporation-condensation and gravity [1]. Thermosyphon can transport heat efficiently over a long distance without any external force and features extreme high equivalent thermal conductivity and isothermal characteristic. Specifically in the super-long distance heat transfer fields, such as the shallow geothermal energy utilization [2], the high efficiency and reliability by thermosyphon make them more attractive heat transfer devices.

Shallow geothermal energy utilizing system employing heat pipe technology was mainly used for de-icing and anti-freezing of special areas, such as airport runway [3], bridges [4] and fire station road [5], and space heating combine with ground source heat pump systems [6]. However, thermosyphon for geothermal utilization has usually a long structure, which is inconvenient to be processed, transported, and installed. In order to overcome these difficulties, our group proposed a kind of polymer composite heat pipe, which was fabricated by thermally conductive polymer with metallic membrane via glue [7]. However, the polymer composite was difficult to be manufactured. In addition, thermosyphon for geothermal utilization have the feature of large aspect ratio and high liquid column due to the long structure. The hydrostatic pressure of high liquid column inhibits the boiling of working fluid at the bottom part of thermosyphon and has a negatively influence on the thermal performance [8, 9].

In order to overcome these difficulties mentioned above, our group proposes a kind of super-long flexible heat pipe with corrugated configuration, expecting the folds at the pipe wall to decrease liquid pool height. The temperature variation of shallow layer ground in Nanjing

Selection and peer-review under responsibility of the scientific committee of the 12th Int. Conf. on Applied Energy (ICAE2020).

city and the feasibility of geothermal utilization by SFHP were analyzed. In addition, the heat transfer characteristics of SFHP were also investigated.

2. EXPERIMENTAL SET-UP AND PROCEDURES

The schematic diagram of the experimental system is illustrated in Fig.1. The SFHP used in the present study is made of stainless steel with 32m length. The structure of SFHP with 30m long is employed corrugated pipe with a 32mm outside diameter and 20mm inner diameter, and the corrugation configuration is U-shaped. A smooth straight tube with a length of 2m, an outer diameter of 22mm and a thickness of 1.5mm is connected with corrugated pipe. The working fluid is selected as ammonia and the filling ratio is 37% (working fluid volume/corrugated pipe volume) [9]. The tested borehole with 60m depth and diameter of 100mm located at the Nanjing city. The corrugated pipe, which consists of an evaporator section of length 28m and 2m long adiabatic section, is vertically placed in borehole. The straight tube of SFHP is regarded as condenser section. A polyethylene tube is employed as water jacket, with a 50mm diameter and a thickness of 2mm. Fourteen T-type thermocouples were used to monitor the temperature at various locations. Ten thermocouples(T_1-T_{10}) were placed in the outer wall of SFHP, as shown in Fig.1(b). Two thermocouples (T_{in}, T_{out}) were applied to measure the inlet and outlet temperature from the water jacket. A thermocouple (T_{50}) setting in the 50m depth below ground surface was used to obtain the ground temperature of the constant temperature zone. In addition, the ambient temperature was measured by the thermocouple (T_a).

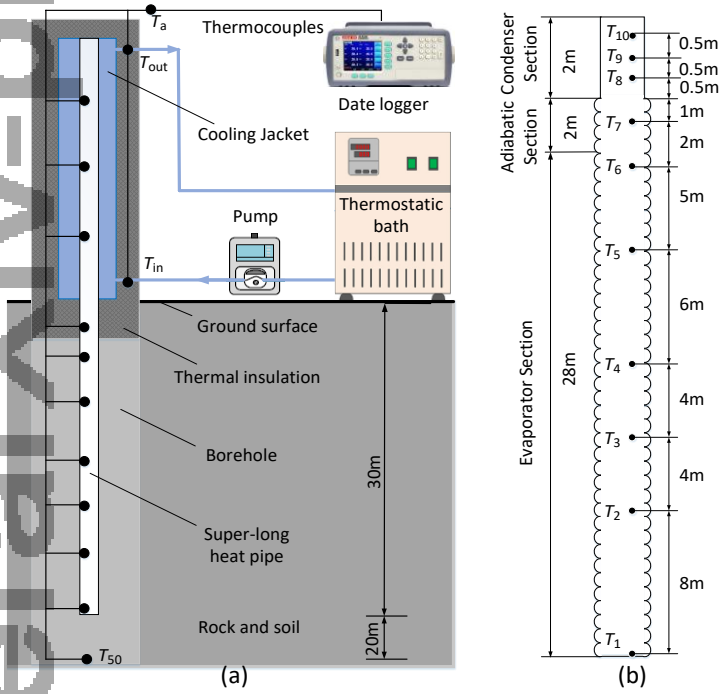

Fig.1. (a) Schematic view of the test platform, (b) Arrangement of temperature monitoring points.

In this study, rock and soil was used as a heat source to supply heat to evaporator. The adiabatic and condenser sections were surrounded by several layers of polymer insulation to minimize the effect of ambient environment. A peristaltic pump (Kamoer, LabUIP-S25-3) with the flow rate accuracy of ±1% was used to measure the flow rate of cooling water. A thermostatic bath (Henglong, DC-1015) with an accuracy of ±0.1℃ was utilized to maintain the inlet temperature of the cooling water at the required temperature. The thermocouples were connected to the data logger (Anbai, AT4532) at the frequency of 0.2Hz to transfer their readings to a u-disk memorizer.

3. DATA REDUCTION AND ERROR ANALYSIS

The heat transfer power and thermal resistance are employed here to evaluate the heat transfer performance at steady-state. The heat transfer power Q in the condenser section is obtained from the following relation:

$$Q = c_p \rho v_{cooling} (T_{co} - T_{ci}) \qquad (1)$$

Where c_p denotes the specific heat of cooling water, ρ is the density of water and $v_{cooling}$ represents the flow rate of cooling water. T_{co} and T_{ci} are the water temperature at the outlet and inlet of cooling jacket respectively.

The overall thermal resistance R_t can be calculated using the following equations:

$$R_t = \frac{T_{e,\,ave} - T_{c,\,ave}}{Q} \qquad (2)$$

where $T_{e,\,ave}$ and $T_{c,\,ave}$ are the average wall temperature of the evaporator and condenser section at steady-state about 10min, respectively.

The relative errors of heat transfer rate and thermal resistance can be evaluated by

$$E(Q) = \sqrt{\frac{d^2(\Delta T_{co\text{-}ci})}{\Delta T_{co\text{-}ci}^2} + \frac{d^2 v_{cooling}}{v_{cooling}^2}} \qquad (3)$$

$$E(R) = \sqrt{\frac{d^2(\Delta T)}{\Delta T^2} + \frac{d^2 Q}{Q^2}} \qquad (4)$$

Where $d(\Delta T_{co\text{-}ci})$, $dv_{cooling}$, $d(\Delta T)$ denote the measurement error of temperature difference between outlet and inlet cooling water, the water flow rate and the temperature difference between wall surface,

respectively. $\mathrm{d}Q$ is the absolute error of Q. $E(Q)$ and $E(R)$ are lower than 7%.

4 RESULTS AND DISCUSSION

4.1 Temperature response and feasibility analysis

Unground temperature is different under degrees of latitude, land-sea distribution, seasonal and diurnal variation. The shallow layer geotemperature variations in Nanjing city and the operation situation of thermosyphon were analyzed from Dec. 5th, 2018 to Sep. 5th, 2020, investigating on the feasibility of this scheme. Before Oct. 19th, 2019, insulation measures were not arranged around adiabatic section, and the condenser section was surrounded by only 20 mm polymer insulation, without cooling jacket. The variations of temperature at out wall surface of SFHP and ambient air temperature are shown in Fig.2. It can be seen from Fig.2 that ground temperature below 10m depth (T_1-T_4、T_{50}) is all-year stabilized on 17-18℃ and has the potentiality for shallow geothermal utilization. Ground temperature above 10m depth(T_5-T_7) change with the fluctuation of ambient air temperature and also exist time difference. The nearer the ground surface, the greater the influence of ground temperature. In summer, as observed in Fig.2, T_7 increased to peak of 27.5℃ at Aug. 10th, 2019 and T_5 reached the peak of 23.9℃ at Sep. 15th, 2020. This phenomenon can be considered the influence of thermal radiation.

It is interesting to note from Fig.2 that the line of $T_{c,ave}$ nearly coincides with the line of T_a during every summer, but was higher during every winter. This phenomenon can be attributed to the discontinuous operation of the SFHP. In winter (Dec. to Mar.), especially when T_a is lower than 5℃, $T_{c,ave}$ is obviously higher than T_a, and SFHP operated automatically. The variation curve of $T_{c,ave}$ and T_a are basically in coincidence when T_a is higher than 15℃, and SFHP was no longer operating. The results indicated that the scheme of geothermal utilization by SFHP is feasible.

4.2 Heat transfer characteristics of SFHP

4.2.1 Thermal performance at steady state

Under the heat transfer test, the inlet cooling water temperature varying the range of 5.5℃ to 9.5℃ with the step of 1℃. Fig.3 show the variation of heat transfer power Q and overall thermal resistance R_t under various cooling water flow rates $q_{cooling}$, from 300ml/min to 600ml/min. It can be seen from Fig.3 (a) that the maximum heat transfer power is 168.3W and the minimum is 84.1W. The relationship between Q and cooling water temperature $T_{cooling}$ is approximate linear dependence. Q decreases with increasing $T_{cooling}$ under the same $q_{cooling}$. But $q_{cooling}$ has an insignificant influence on the heat transfer power. Fig.3(b) shows that R_t increases with increasing $T_{cooling}$ when $q_{cooling}$ maintains constant value. Furthermore, $q_{cooling}$ has a significant influence on R_t, which decreases with decreasing $q_{cooling}$. But the effect is thinner when $q_{cooling}$ is higher than 500ml/min.

4.2.2 Start-up characteristics

The start-up characteristics of heat pipe can be reflected by wall temperature response at start-up state. Before the start-up testing, no cooling water enter the jacket. The variation of temperature at outer surface of SFHP under various cooling water flow rate are shown in Fig.4. The inlet temperature of cooling water was

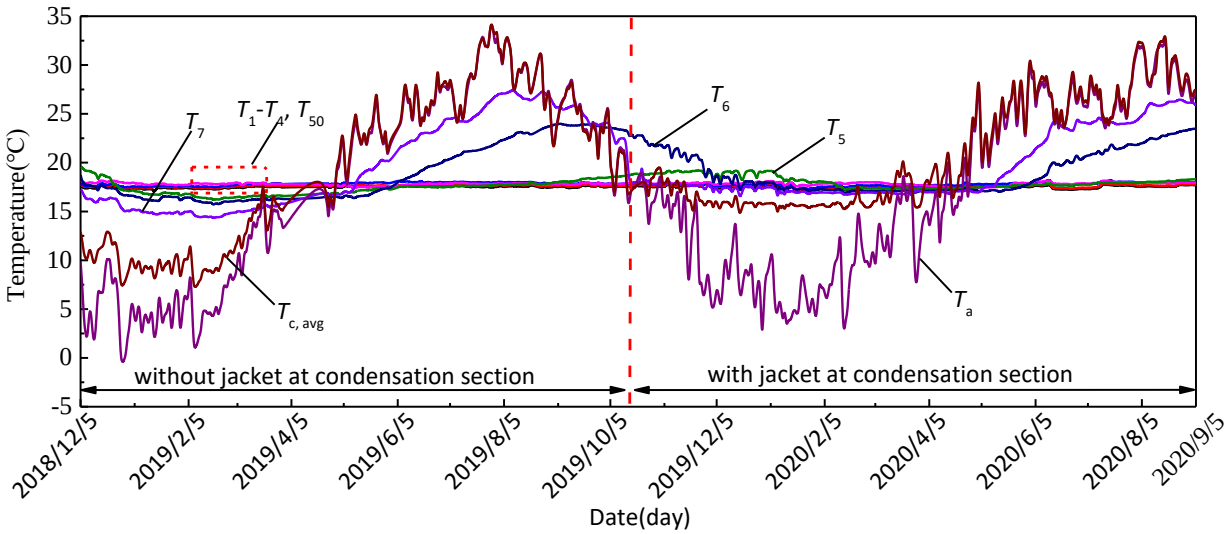

Fig 2. Variations of ambient air temperature and temperature on the outer wall of SFHP.

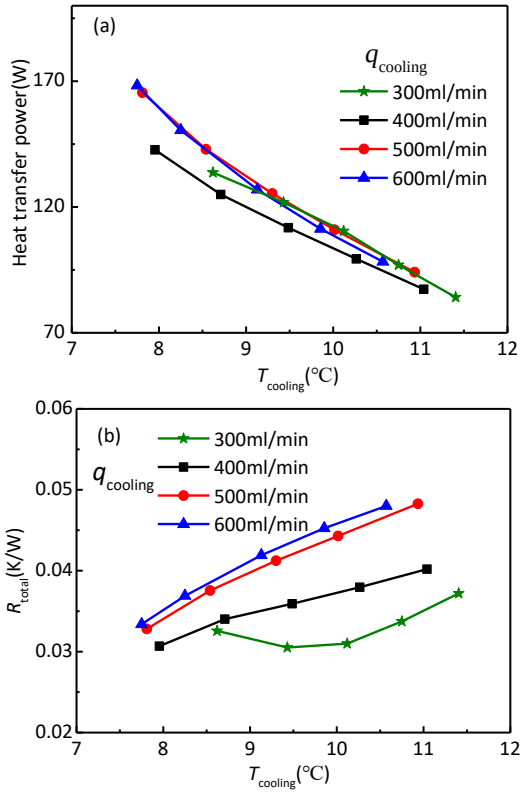

Fig 3. The effects of flow rate and temperature of cooling water on steady thermal performance: (a) Heat transfer power, (b) Total thermal resistance.

maintained at 5.5℃ in this section. The wall temperature of condenser (from the bottom up) decrease quickly after entering cooling water to jacket. After a few time,

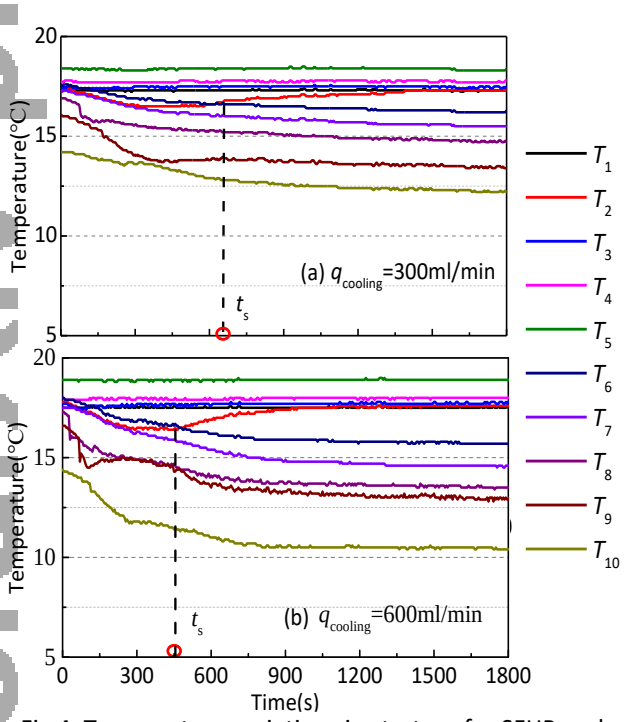

Fig 4. Temperature variations in start-up for SFHP under various flow rates of cooling water.

T_6 and T_7 also decrease similarily to wall temperature of condenser. Working fluid in the condenser condense when the cooling water enter jacket, subsequently, liquor condensate downflow along inner wall surface by gravity. With ammonia vapours condensate continuously, vapor pressure of inner chamber decreases and the corresponding saturation temperature also decreases. Ammonia occurs intense boiling when attaining the initial boiling superheat. T_2 decreases to a minimum value and remains stable for a while. When T_2 begin to increase, the SFHP is considered to start completely, and the time taken is defined as the start-up time t_s. It can be seen from Fig.4 that t_s is shortened with the increase of cooling water flow rate. When $q_{cooling}$ equals to 300ml/min, 650 seconds are needed, but it's only about 450 seconds with $q_{cooling}$ at 600ml/min.

5 CONCLUSIONS

In this paper, the temperature response characteristics of SFHP were experimentally investigated. Steady-state and start-up thermal performance were also studied. The main conclusions are shown as follow:

(1) The underground areas deeper than 10m has the potentiality for shallow geothermal utilization and the scheme of geothermal utilization by SFHP is feasible.

(2) The temperature of cooling water has a significant effect on thermal performance at steady-state. The maximum heat transfer power is approximately 168.3W under the condition that the temperature of cooling water is 8.5℃.

(3) The start-up time of the SFHP is shortened with increasing flow rate of cooling water.

ACKNOWLEDGEMENT

It is gratefully acknowledged that this work is supported by the "National Natural Science Foundation of China" [grant number 51906101].

REFERENCE

[1] Fadhl B, Wrobel LC, Jouhara H. CFD modelling of a two-phase closed thermosyphon charged with R134a and R404a. APPL THERM ENG. 2015;78:482-490.

[2] Li X, Li J, Zhou G, Lv L. Quantitative analysis of passive seasonal cold storage with a two-phase closed thermosyphon. APPL ENERG. 2020;260:114250.

[3] Chi Z, Yiqiu T, Fengchen C, Qing Y, Huining X. Long-term thermal analysis of an airfield-runway snow-melting system utilizing heat-pipe technology. ENERG CONVERS MANAGE. 2019;186:473-486.

[4] Won J, Kim C, Lee S, Lee J, Kim R. Thermal characteristics of a conductive cement-based composite for a snow-melting heated pavement system. COMPOS STRUCT. 2014;118:106-111.
[5] Zorn R SHKT, "De-Icing and Snow Melting System with Innovative Heat Pipe Technology," in Proceedings World Geothermal Congress, (Melbourne, Australia, 2015).
[6] Wang X, Wang Y, Wang Z, Liu Y, Zhu Y, Chen H. Simulation-based analysis of a ground source heat pump system using super-long flexible heat pipes coupled borehole heat exchanger during heating season. ENERG CONVERS MANAGE. 2018;164:132-143.
[7] Wang X, Zhu Y, Zhu M, Zhu Y, Fan H, Wang Y. Thermal analysis and optimization of an ice and snow melting system using geothermy by super-long flexible heat pipes. APPL THERM ENG. 2017;112:1353-1363.
[8] Seo J, Lee J. Length effect on entrainment limitation of vertical wickless heat pipe. INT J HEAT MASS TRAN. 2016;101:373-378.
[9] Wang X, Liu H, Wang Y, Zhu Y. CFD simulation of dynamic heat transfer behaviors in super-long thermosyphons for shallow geothermal application. APPL THERM ENG. 2020;174:115295.